Response to reviewer 2

We thank the reviewer for his/her time, the thoughtful suggestions and helpful comments. Guided by the two reviewers' remarks the paper has been corrected and revised. In the following we provide point-by-point responses to the reviewer's suggestions. His/her remarks are set in italics, our answers are added in normal font. The revised text is indented.

[...] However, a better experimental design and perhaps better site selection are needed to produce more impactful results. The main conclusions of this paper are not really new, at least qualitatively. In addition, one issue I have is with the implementation of its O/L tracking (see comment 3 below) and how this would affect the results quantitatively and how this would translate to the spaceborne case. Overall, I think the paper can be suitable for publication, provided that the comments are adequately addressed and that the paper is viewed as a "pathfinder" for future experiments.

The main design criteria of the present study were twofold. First, the set-up should be based on a receiver software implementation available in source code format, to allow us complete control over all details of the open-loop signal tracking. Second, the project had to be accommodated within limited budget allocated to this activity. We agree that both, experimental design and measurement site selection could be improved and these modifications would most certainly lead to more relevant results. We intend to continue this line of research and hope to gather sufficient funding support for an optimized measurement set-up. The present submission is part of this effort.

And we fully agree that the "GLESER" campaign should be viewed as a pathfinder for future, more refined experiments with the objective to exploit the information content of low elevation GNSS data in the best possible way.

(1) The paper should be made more succinct. In particular, the detailed description of the OpenGPS receiver does not offer much insight into understanding the data. The readers have to wade through too much background materials before getting to the results. I suggest significant shortening of Section 2.2 and Section 2.3. Another option is to move the materials to an Appendix.

We agree that sections 2.2 and 2.3 are rather technical; in the revsied

manuscript both sections are shifted to the appendix.

(2) L15:
it states that "vertical refractivity gradients ... correlate moderately well with observed signal amplitude fluctuations ..." However, Figure 16 shows that only 3 out of 9 cases "yield significant correlations". I suggest changing the wording of "correlate moderately well" to better represent the results.

We accept the criticism, that our original approach, to understand the observed C/N_0 fluctuations, is too simplistic and is not convincing. Following a suggestion made by the first reviewer, Multiple Phase Screen (MPS) simulations of signal propagation at the low elevation angles have been performed to support the analysis of the C/N_0 variations.

The revised version of the paper contains the following new section as suggested by reviewer 1:

Simulations

In order to support the interpretation of the observed C/N_0 fluctuations we performed a series of Multiple Phase Screen simulations (Knepp, 1983; Martin and Flatté, 1988; Grimault, 1998). The propagation of a plane wave through the lower troposphere is modeled by a series of 500 non-equidistant phase screens ranging from the receiver location to a distance of 500 km. On each phase screen the wave suffers a phase delay determined by the interscreen distance Δz and the refractivity height profile (Sokolovskiy, 2001)

$$N(h) = 400 \exp\left(\frac{-h}{h_s}\right) \left(1 - 0.05 \frac{2}{\pi} \operatorname{atan}\left(\frac{h - h_{tp}}{h_{zn}}\right)\right) \tag{1}$$

with scale height $h_s = 8$ km, planetary boundary layer (PBL) top height h_{tp} and PBL top transition zone $h_{zn} = 50$ m. The interaction of the wave with the ground surface is modelled by applying a raised-cosine filter with a 6 dB steepness of 25 m (i.e., within 25 m the filter weight decreases by 6 dB) at zero altitude. The phase screens extend from -20 km to $+20$ km with a 5 km wide raised-cosine filter applied at the upper and lower boundary to suppress spurious diffraction effects; the receiver altitude is taken to be 50 m. The variation of elevation angle between $-2°$ and $+2°$ is modelled by tilting the ground surface and its overlying atmosphere correspondly.

Results from four simulation runs are shown in fig. 1; it displays the normalized signal amplitude as a function of elevation angle. Signal absorption at the ground surface produces characteristic diffraction

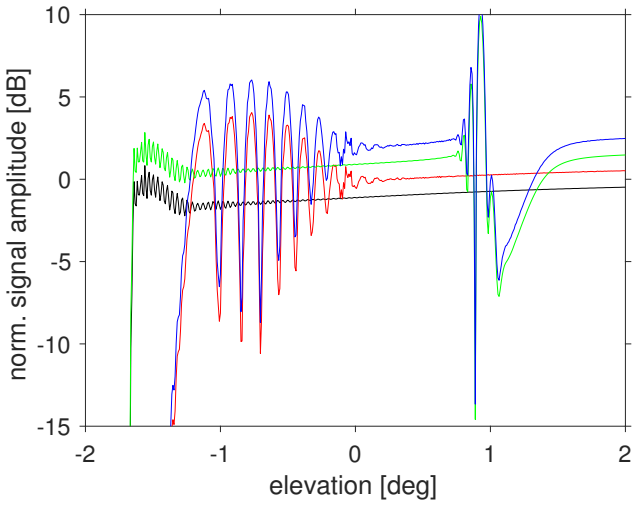

Figure 1: Normalized signal amplitudes as a function of elevation angle derived from several Multiple Phase Screen simulations. Refractivities on the individual phase screens are calculated from an exponential profile furnished with a planetary boundary layer in the lower troposphere. Signal absorption at the surface is taken into account (red and blue lines), green and black lines show the result without ground absorption. Two boundary layers are modelled: a horizontal boundary layer top at 2 km altitude (red and black) and a layer top increasing from 1 km to 2 km between 30 and about 60 km distance from the receiver (blue and green). For legibility the red, green and blue lines are shifted by an additional +1 dB, +2 dB and +3 dB offset, respectively. For details see text.

patterns for elevation angels below 0° (red and blue lines). Without ground absorption the diffraction patterns almost disappear and the profiles resemble step functions expected from geometric optics (green and black). The simulations did not produce C/N_0 fluctuations for horizontally oriented PBL tops (parameterized by h_{tp} in eqn. 1). However, if the top layer tilts towards the receiver, substantial signal deviations at elevation angles above 0° are observed. Fig. 1 illustrates this phenomenon for a PBL top layer ascending from 1 km at 30 km distance to 2 km at about 60 km (green and blue lines); below 30 km and above 60 km h_{tp} remains fixed at 1 km and 2 km, respectively.

The MPS simulation results plotted in fig. 1 indicate ground effects below about 0° elevation angle (blue and red) and PBL-induced C/N_0 variations above about 0° (blue and green). The results suggest that these C/N_0 fluctuations are independent from each other and tend to be separated in elevation angle space. Finally, we note that the

addition of irregularities on spatial scales characteristic for turbulence to the refractivity profiles did not produce significant C/N_0 changes.

(3) L245-255:
the O/L tracking models are extrapolated from the C/L tracking data at higher elevation angles. Thus one can argue that this is more similar to the "flywheel-ing" algorithm implemented on CHAMP and SAC-C and might not work well under some conditions (which the authors recognized, see L267-270). Please explain/justify why it is done this way. Is it possible to use an a priori O/L model as was done in COSMIC and Metop/GRAS?

We agree that our open-loop implementation shares certain features of "fly-wheeling" signal tracking as decribed in Ao et al. (2003) On the other hand, questions regarding the precise differences between "fly-wheeling" and O/L are difficult to answer without access to implementation details, i.e. source code. We decided to classify our implementation as "open-loop" tracking, because the "OpenGPS" instrument outputs inphase/quadphase correlation sums together with NCO phases when O/L tracking is activated. CHAMP "fly-wheeling" raw data do not provide this information; thus, based on the CHAMP raw data analysis it cannot be unambiguously concluded that the carrier tracking loops were fully opened in "fly-wheeling" mode.

It is certainly possible for "OpenGPS" (and will be considered for future implementations) to use "fixed" a-priori O/L models as implemented COSMIC and Metop/GRAS. However, it should be emphasized that owing to the closed architecture of the COSMIC and Metop/GRAS receivers (and hardware related differences) an exact emulation appears not feasible.

We suppose that a) details of the receiver firmware are relevant for the scientific data evaluation of RO observations and b) certain specific (admittedly detailed) questions on RO data can only be conclusively answered on the source code level of the tracking software. For this reason we make available the OpenGPS receiver source code (as part of the "GLESER" raw data archive). It can be accessed via the Digital Object Identifier (DOI) doi:10.5880/GFZ.2016.1.1.002.

(4) Eqs (6)-(8):
is there a reference for calculating C/N0 this way? I am confused with Eq. (8) since this apparently yields a noise floor of 17 dB Hz that depends only on the integration time. Shouldn't this depend on the antenna gain, cable loss, etc.?

Suitable references are Badke (2009); Kaplan (1996); Parkinson and Spilker (1996). Most likely the misunderstanding is caused by our usage of the term "noise floor" for the C/N_0 value of 17 dB Hz. C/N_0 is the carrier signal-to-

noise density ratio and as such does not provide information on the noise measured by the receiver front-end. The value of 17 dB Hz represents the C/N_0 value with the signal completely blocked by the horizon. According to eqn. 6 this value depends only on the chosen coherent integration time T_c. In the revised version the misleading term "noise floor" has been removed.

(5) Table 1:
PRN28 yields anomalously low (about 35%) O/L enhancement. Any idea why?

Our open-loop implementation rests on the assumption that for elevation angles between 0 and +2° signal tracking is stable without strong C/N_0 fluctuations. The low O/L enhancement for PRN28 suggests that this assumption is invalid in this instance.

The revised version of paper includes the paragraph (figure number 4, mentioned in the text, refers to the submitted paper, not the present document):

> The low O/L enhancement values for PRN 28 might be caused by signal reflections at the water surface of Templiner lake (see fig. 4 at about 260° azimuth angle). As described in the appendix (subsection A2), the O/L model is initialized within the elevation angle range between 0° and +2°. It appears feasible that surface reflections induce C/N_0 fluctuations at these elevation angles degrading the quality of the O/L model and thereby causing poor O/L performance.

(6) Fig. 15:
I suggest more distinct colors for the light blue and dark blue lines. I have a hard time distinguishing them. It is also hard to tell the actual values of frequency offsets from these plots. I think it would be useful to have a summary table of mean and standard deviation of Δf_{obs} as a function of C/N0 that average over all 9 PRNs.

In the revised paper a better line coloring is used (see fig. 2) and a summary table showing the mean and standard deviation of Δf_{obs} as a function of C/N_0 is included (see table 1; the figure numbers mentioned in the figure and table captions refer to the submitted paper, not the present document).

(7) L522:
Is the refractivity based on ECMWF at a grid point closest to the receiver? How about temporal differences? How does the refractivity vary along the ray paths? Besides vertical refractivity, horizontal inhomogeneity and small-scale irregularities (turbulence) can also lead to strong signal fluctuations. These effects could perhaps explain the lack of correlations for many of the PRNs.

Table 1: Mean and standard deviations of Δf_{obs} (center column) for nine values of the carrier signal-to-noise density ratio $\mathrm{C/N_0}$ between 10 and 50 dB Hz; averaging bin size is 5 dB Hz. The statistics is based on all PRNs shown in fig. 15. The third column gives the corresponding result neglecting frequency deviations larger than 40 Hz.

$\mathrm{C/N_0}$ [dB Hz]	Δf_{obs} [Hz]	$\Delta f_{\mathrm{obs}}^{<40\,\mathrm{Hz}}$ [Hz]
10	8.23 ± 18.08	4.51 ± 14.01
15	5.48 ± 15.47	1.85 ± 9.68
20	2.75 ± 11.50	0.50 ± 5.68
25	1.28 ± 7.89	0.19 ± 3.29
30	1.23 ± 7.71	0.08 ± 1.96
35	1.39 ± 8.17	0.06 ± 1.38
40	0.95 ± 6.78	0.04 ± 1.12
45	0.62 ± 5.47	0.05 ± 1.28
50	0.56 ± 5.23	0.06 ± 1.68

In the orginal version of the paper the closest ECMWF grid point was selected, which is about 42 km south of the receiver location. In the revised analysis an alternative approach was followed and grid points oriented towards western directions were chosen (see below).

Following a suggestion by reviewer 1 we performed provisional Multiple Phase Screen (MPS) simulations to support the interpretation of the observed $\mathrm{C/N_0}$ profiles, in particular the observed $\mathrm{C/N_0}$ fluctuations. The revised paper includes an additional section and figures describing the MPS results (see response to specific comment below). We note, that our MPS simulations failed to produce significant $\mathrm{C/N_0}$ fluctuations if irregularities on spatial scales characteristic for turbulence were added to the refractivity profiles.

The revised section describing the correlation between the observed $\mathrm{C/N_0}$ fluctuations and ECMWF-derived refractivity gradients reads as follows:

> The MPS simulations (fig. 1) suggest that at negative elevation angles diffraction effects caused by the ground surface dominate the observed $\mathrm{C/N_0}$ fluctuations. At higher elevations atmospheric multipath seems to be more relevant. This hypothesis is tested for the six month time period from March to August 2014 by correlating the standard deviation of $\mathrm{C/N_0}$ between elevation angles of $+1^\circ$ and $+2^\circ$ with the mean refractivity gradient $\langle dN/dz \rangle$. The calculation of $\langle dN/dz \rangle$ is restricted to the altitude range from 1 to 3 km. Fig. 3 shows the results for nine

PRNs.

The vertical refractivity profiles $N(z)$ are extracted from European Centre for Medium-Range Weather Forecasts (ECMWF) meteorological fields. Their horizontal resolution is $1^\circ \times 1^\circ$ (about 110 km in meridional and 69 km in zonal direction at the receiver location) with 137 height levels ranging from 0 to about 80 km; the averaging interval of 1 to 3 km corresponds to about 13 vertical height levels. For signal azimuth angles less than -90° (west to south-west) the refractivity profile is extracted from ECMWF grid point (52°N, 12°E), about 84.4 km south-west of the observation site (-119.8° true bearing). For azimuth angles greater than -90° (west to north-west) the ECMWF grid point (53°N, 12°E) is selected, which is located about 99.8 km in the north-western direction (-45.8° true bearing). The standard deviation of the carrier signal-to-noise density ratio, $\sigma(\mathrm{C/N_0})$, calculated within the elevation angle range $+1^\circ < \epsilon < +2^\circ$, is taken as proxy for the signal amplitude fluctuation.

Each panel of fig. 3 includes information on the correlation; the Pearson and Spearman coefficients are quoted in the top and bottom line, respectively, (see, e.g., Press et al., 1992); the corresponding significance parameters are given in brackets. The numerical values indicate that $\langle dN/dz \rangle$ and the standard deviation of $\mathrm{C/N_0}$ are weakly to moderately correlated. With the exception of PRN 17 (top right panel) all calculated correlations are significant on the 5% level. The (negative) correlations range from -0.17 to -0.40. We note that ECMWF refractivity profiles below 1 km frequently exhibit strong gradients. Their inclusion into the calculation of $\langle dN/dz \rangle$ significantly decreases the correlations or even renders them insignificant.

The MPS simulations (see fig. 1) also suggests that the (negative) correlation between $\sigma\,(\mathrm{C/N_0})$ and $\langle dN/dz \rangle$ weakens if elevation angles close to or below the horizon are included. The data displayed in fig. 4 confirms this prediction. It shows the correlation between $\sigma\,(\mathrm{C/N_0})$ and $\langle dN/dz \rangle$, however in this case the elevation angle range used for the calculation of $\sigma\,(\mathrm{C/N_0})$ is extended downwards to -2°. Comparison with fig. 3 shows that (with the exception of PRN 7 and the Pearson coefficient of PRN 18) the derived correlations are no longer significant, i.e. based on these results the null hypothesis cannot be rejected on the 5% significance level.

(8)
Do you expect local environmental effects (e.g., local multipath) and ionospheric conditions to have significant impact on the measurements?

Ionospheric refraction and multipath certainly has an effect on the observed code delays and carrier phases. It is very well possible, that these phenomena cause C/N_0 fluctuations as well. Since the "OpenGPS" receiver is a single frequency device, there is unfortunately no way extract a definite answer from the measurement data. The neglect of both aspects, local multipath and ionospheric dispersion may partly explain non-perfect correlation listed in fig. 3.

In the revised paper the following sentence is added to the conclusions:

> The present study did not address potential contributions of the ionospheric signal propagation and/or local multipath to the observed C/N_0 fluctuations. These are important issues that need to be addressed in future work preferably using dual frequency receivers.

Finally, we note that the "GLESER" campaign raw data files have been supplied with the digital object identifier doi:10.5880/GFZ.2016.1.1.002 and are available through the DOI resolver `http://dx.doi.org/`. The data are supplemented with a set of documents describing the measurement data files and an archive containing the "OpenGPS" receiver software used during the measurement campaign.

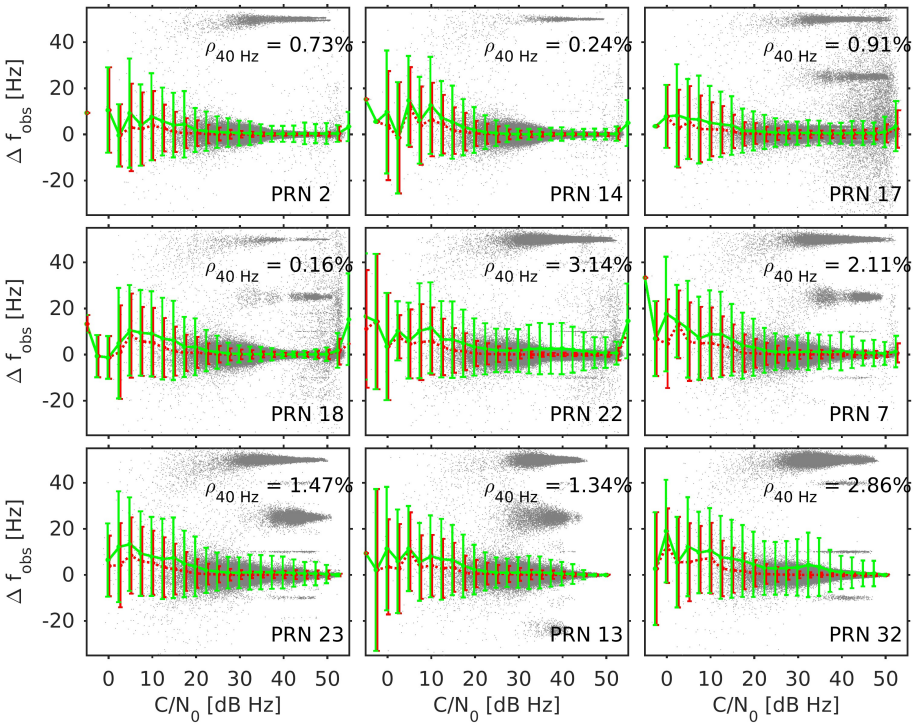

Figure 2: Same as fig. 10, however, showing the difference between the two observed frequencies obtained from O/L channel A and B as a function of the mean signal-to-noise density ratio. Mean and 1-σ standard deviations, calculated from C/N_0 bins 2.5 dB Hz wide, are marked in green. The fraction of data points exceeding $\Delta f_{\mathrm{obs}} > +40$ Hz is indicated as $\rho_{40\,\mathrm{Hz}}$. The result of the statistical analysis excluding this subset still exhibits a positive bias if $C/N_0 \lesssim 30$ dB Hz (red).

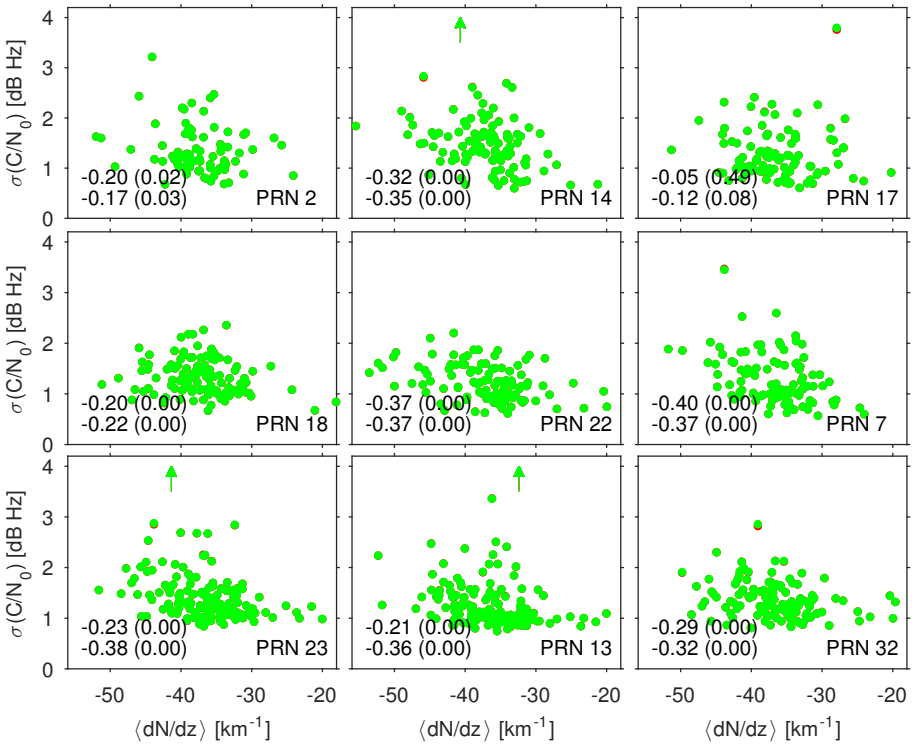

Figure 3: Standard deviation of C/N_0 at elevation angles between $+1°$ and $+2°$ versus mean refractivity gradient for nine PRNs extracted from ECMWF (March–August 2014). For PRN 13, 14 and 23 one data point exceeds the axis limit of 4.2 dB Hz; its respective mean refractivity gradient is marked by an arrow. (Of course, these observations are included in the statistical analysis.) In the lower left corner of each panel correlation coefficients are given (top: Pearson's coefficient, bottom: Spearman's coefficient). The corresponding significance parameters are stated in brackets. Results from O/L channel B (green points) very closely agree with channel A data (red) and therefore almost completely mask the latter.

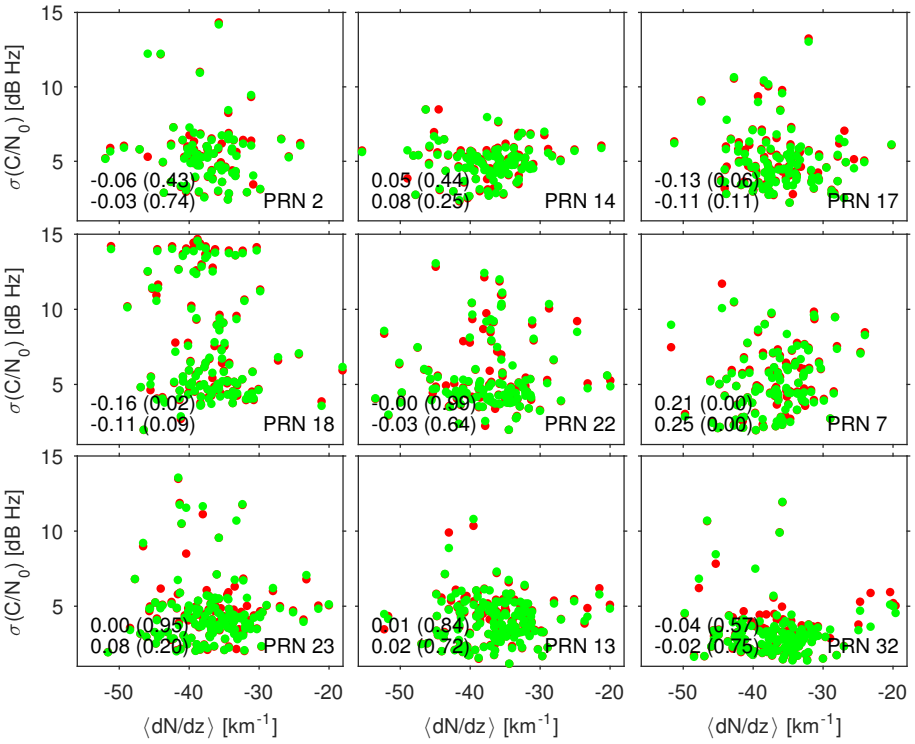

Figure 4: Same as fig. 3, however, the correlation analysis now includes all observations at elevations between $-2°$ and $+2°$. With the exception of PRN 7 (and the Pearson's coefficient for PRN 18) the derived correlations are no longer significant.

Bibliography

Ao, C. O., Meehan, T. K., Hajj, G. A., Mannucci, A. J., and Beyerle, G.: Lower-Troposphere Refractivity Bias in GPS Occultation Retrievals, J. Geophys. Res., 108, 4577, doi:10.1029/2002JD003216, 2003.

Badke, B.: What is C/N_0 and how is it calculated in a GNSS receiver?, InsideGNSS, 4, 20–23, 2009.

Grimault, C.: A multiple phase screen technique for electromagnetic wave propagation through random ionospheric irregularities, Radio Science, 33, 595–605, doi:10.1029/97RS03552, 1998.

Kaplan, E. D.: Understanding GPS: Principles and applications, Artech House, Boston, London, 1996.

Knepp, D. L.: Multiple phase-screen calculation of the temporal behaviour of stochastic waves, Proc. of the IEEE, 71, 722–737, 1983.

Martin, J. M. and Flatté, S. M.: Intensity images and statistics from numerical simulation of wave propagation in 3-D random media, Appl. Opt., 27, 2111–2126, doi:10.1364/AO.27.002111, 1988.

Parkinson, B. W. and Spilker, J. J., eds.: Global Positioning System: Theory & Applications, Volume I&II, Am. Inst. of Aeronautics and Astronautics, Washington, DC, 1996.

Press, W. H., Teucholsky, S. A., Vetterling, W. T., and Flannery, B. P.: Numerical recipies in C, The art of scientific computing, 2nd edition, Cambridge University Press, Cambridge, 1992.

Sokolovskiy, S. V.: Modeling and inverting radio occultation signals in the moist troposphere, Radio Sci., 36, 441–458, doi:10.1029/1999RS002273, 2001.